ARTICLE

S. Portet · J. A. Tuszyński
C. W. V. Hogue · J. M. Dixon

Elastic vibrations in seamless microtubules

Abstract Parameters characterizing elastic properties of microtubules, measured in several recent experiments, reflect an anisotropic character. We describe the microscopic dynamical properties of microtubules using a discrete model based on an appropriate lattice of dimers. Adopting a harmonic approximation for the dimer–dimer interactions and estimating the lattice elastic constants, we make predictions regarding vibration dispersion relations and vibration propagation velocities. Vibration frequencies and velocities are expressed as functions of the elastic constants and of the geometrical characteristics of the microtubules. We show that vibrations which propagate along the protofilament do so significantly faster than those along the helix.

Keywords Microtubule · Microtubule structure · Microtubule dynamics · Lattice · Elastic vibrations

Introduction

Microtubules (MTs) are proteins organized in a network that is interconnected with microfilaments and intermediate filaments to form the cytoskeleton. Each of the protein fibers has specific physical properties and structures suitable for its role in the cell. MTs are long, hollow, cylindrical objects made up of protofilaments interacting laterally, and consisting of longitudinally

S. Portet (✉) · C. W. V. Hogue
The Samuel Lunenfeld Research Institute,
Room 1060, Mount Sinai Hospital,
600 Univercity Avenue, Toronto,
ON, Canada, M5G 1X5
E-mail: sportet@mshri.on.ca

J. A. Tuszyński
Department of Physics, University of Alberta,
Edmonton, AB, Canada, T6G 2J1

J. M. Dixon
Department of Physics, University of Warwick,
Coventry, CV4 7AL, UK

stacked α,β-tubulin heterodimers; longitudinal and lateral bonds exhibit different strengths (VanBuren et al. 2002). In vivo MTs have typically 13 protofilaments but, for example, 15 protofilament MTs are found in *Caenorhabditis elegans*. Unger et al. (1990) observed in vitro MTs with a number of protofilaments ranging from 8 to 16 depending on the assembly conditions. The MT structure can be represented by a helical surface lattice interrupted by mismatches which are called seams (Chrétien and Wade 1991). To accommodate different numbers of protofilaments the whole lattice is rotated to compensate the extra protofilaments and to absorb the mismatch (Ray et al. 1993). In the cell MTs are normally organized in an aster radiating near the nucleus towards the cell periphery. MTs are involved in a number of functions of the cell, such as cell shape maintenance, mitosis and play an important role in intracellular transport. They form the mitotic spindles for the segregation of chromosomes during cell division, and they are supports for directional transport driven by motor proteins. MTs are highly dynamic polymers, characterized, for example, by dynamic instabilities, successive periods of growth and shrinkage. Under specific conditions treadmilling may occur, where addition of heterodimers at one end of an MT and release at the other end take place at the same rate.

There have been a number of experimental studies in recent years dealing with the various aspects of the elasticity of MTs. By biological standards, MTs are rigid polymers with a large persistence length of 6 mm (Boal 2002). From Janmey's experiments (Janmey et al. 1991), MTs suffer a larger strain for a small stress compared with either microfilaments or intermediate filaments. The rupture stress for MTs is very small and typically is only about 0.4–0.5 N/m^2 (Janmey et al. 1991). From the literature, we can observe that the shear and Young's moduli are significantly different, which reflects structural anisotropy of the material (Kis et al. 2002). An anisotropic material has physical characteristics with different values when measurements are made in several directions within the same material: e.g., values of the

Young's modulus ranging from 10^6 to 10^9 N/m^2 can be found in the literature (Kis et al. 2002; Tolomeo and Holley 1997).

A few already available dynamical elastic properties of MTs are listed in Table 1 although many more are still to be determined. In connection with this it is worth noting that there are several papers in the literature dealing with static and elastic properties (Jánosi et al. 1998) and the vibrational properties of cytoskeleton filaments and, in particular, MT vibrations. Elastic vibrations of subunits around their equilibrium positions in a lattice have been called phonons in the literature (Pokorny et al. 1997; Sirenko et al. 1996b).

Sirenko et al. (1996b) studied theoretically the vibrational properties of MTs by adopting a continuum medium approximation in cylindrical geometry for an isotropic material. By describing filaments as elastic shells immersed in water, they identified several modes of vibration—radial, torsional and longitudinal—with the attendant dispersion relations. Their predicted phonon velocities ranged from approximately 200 to 600 m/s. In a sequel paper (Sirenko et al. 1996a) these authors arrived at a higher estimate of the phonon velocities, namely 800–1,300 m/s. They also predicted the existence of an infinite set of helical waves with parabolic dispersion relations. While these results are very useful in identifying the most likely modes of vibrational propagation, they still await experimental confirmation. The structure of MTs is highly heterogeneous, and both experimental measurements and theoretical analyses indicate a highly anisotropic dynamical picture (Kis et al. 2002). Thus, we believe that a discrete approach is not only adequate, but it also allows the expression of MT structural anisotropy in a natural way.

Pokorny et al. (1997) attempted to find dispersion relations based on a monatomic linear chain model representing individual protofilaments made up of monomers, and by using additivity properties they described an MT and concluded that phonon frequencies in the range 10^7–10^{10} 1/s can be expected. They also showed that the energy can be supplied by the hydrolysis of GTP.

Our approach will go further than the work of Pokorny et al. (1997) by modeling the structure of MTs by a cylinder unfolded into a planar *lattice of tubulin dimers* satisfying appropriate boundary conditions in accordance with the essential geometrical properties of MTs. The structural transformation to accommodate different numbers of protofilaments is the rotation of the whole lattice (Chrétien and Wade 1991), without modifying the interprotofilament interactions. Consequently the *local* geometry of the lattice, (i.e., longitudinal and lateral interactions between dimers) is preserved. Hence, from the canonical lattice describing a 13-protofilament MT, we deduce the general dimensions of the lattice of dimers representing an MT independently of the number of protofilaments. From this lattice, we develop a microscopic model of classical vibration modes to study the dynamics of dimers within the MT surface (excluding radial oscillations). We estimate dispersion relations by using heterogeneous elastic coefficients that reflect the anisotropic character of MTs. The elastic coefficient values are obtained from molecular dynamics simulations of tubulin–tubulin interactions (Sept et al. 2003) and from experimental data (de Pablo et al. 2003). Our predicted vibration frequencies and corresponding velocities, which are expressed as functions of elastic constants and structural properties of MTs, are in the same range as those estimated by Sirenko et al. (1996a, 1996b), and slightly larger than those estimated by Pokorny et al. (1997). Although no experiments have yet been performed to validate these predictions, they are clearly within today's experimental capabilities. Thus, by using recently published information regarding elastic properties and the molecular geometry of MTs we describe at a microscopic level the dynamical elastic properties of MTs by accounting for their anisotropy.

Modeling

In the literature, theoretical and experimental data can be found for an MT description using a lattice of monomers (Amos 1995; Chrétien and Wade 1991), but rarely by a lattice of dimers (Metoz and Wade 1997). Chrétien and coworkers (1991, 1998) have given precise descriptions of MT structures in terms of a surface lattice composed of tubulin monomers in the *lattice accommodation model*. In an MT with 13 protofilaments, the protofilaments are parallel to the MT axis forming a hollow cylinder (Chrétien and Wade 1991). Tubulin monomers are longitudinally aligned to form the protofilaments; the monomer spacing along the protofilament is $b = 4.05$ nm (Chrétien et al. 1998). Each protofilament is shifted lengthwise with respect to its neighbour describing left-handed helical pathways running around the MT surface. The longitudinal shift between monomers of adjacent protofilaments is $e = 0.935$ nm (Chrétien et al. 1998). The accumulated circumferential shift is 13×0.935 nm, which is equal to a helix pitch of 3×4.05 nm, indicating that three helices of monomers are necessary to describe the whole MT surface (Chrétien et al. 1998). The separation between protofilaments is $d = 5.13$ nm (Chrétien et al. 1998). The 13-protofilament and 3-start helix MT is the so-called canonical MT.

There exists an important variability in the number of protofilaments (Unger et al. 1990). MTs accommodate different numbers of protofilaments by skewing their protofilaments (Langford 1980), without modifying their lateral interactions. The structural alteration is

Table 1 Dynamical elastic properties of microtubules (*MTs*)

Phonon frequencies	10^7–10^{10} 1/s (Pokorny et al. (1997)
Phonon velocities	200–600 m/s (Sirenko et al. 1996b)
	100–1,000 m/s (Pokorny et al. 1997)
	800–1,300 m/s (Sirenko et al. 1996a)

equivalent to the rotation of the whole protofilament sheet by an angle θ that can be expressed as a function of the number of protofilaments N, the number of helices S constituting the MT, the separation between protofilaments d, the longitudinal shift between adjacent protofilaments e, and the spacing between subunits b (Chrétien et al. 1998):

$$\tan\theta = \frac{1}{d}\left(\frac{Sb}{N} - e\right). \tag{1}$$

Thus, the interactions between protofilaments are locally preserved in MTs. In other words, the local geometry, i.e., the subunit neighbourhood geometry, is independent of the protofilament numbers (Ray et al. 1993). The number of protofilaments only influences the MT radius r (see Fig. 7 in Chrétien et al. 1998) and the skew angle θ. Hence, the local geometry of the subunit neighbourhood can be deduced from the geometry of the canonical MT.

To study the dimer vibrations inside the MT wall, we use a lattice model of dimers which is considered to be a series of coupled oscillators whose equilibrium positions represent the geometry of the MT.

Lattice of dimers

The longitudinal interdimer interactions are very similar to those between monomers within a dimer. However, an extra electrostatic interaction exists between monomers that does not occur between dimers. This component affects the strength of longitudinal intradimer interactions (Nogales 1999), which are stronger than longitudinal interdimer interactions (Nogales et al. 1999). Furthermore, the basic subunit for the MT assembly is not the monomer but the dimer. Consequently, we assume longitudinal intradimer interactions to be structurally stable inside the MT wall, and we investigate the vibration dynamics of dimers inside the MT surface.

A seamless MT can be modeled as a three-dimensional helical lattice of *dimers* (Fig. 1a) (Metoz and Wade 1997). We consider dimers as points at their centers of mass (Fig. 1b). The pitch of helices that run around the MT wall is proportional to the equilibrium distance, b, between adjacent dimers along a protofilament. Hence pitch is equal to Sb, where S represents the number of helices necessary to describe a whole MT surface (Fig. 1b). Helices are well defined by a pitch, Sb, and a radius, r, and are characterized by the radius of curvature expressed as $r\left[1 + (Sb/2\pi r)^2\right]$. From helical geometry, we can calculate the dimensions of the dimer neighbourhood in the lattice.

We open the three-dimensional lattice along the length of a protofilament, parallel to the MT axis as we consider a 13-protofilament MT, and unroll it to obtain a two-dimensional planar lattice of dimers. The characteristic dimensions of the two-dimensional planar lattice arise directly from the three-dimensional lattice geometry; hence, all equilibrium angles and distances between neighbouring dimers are preserved (Figs. 1c, 2a). By construction and from the radius of curvature of helices, we obtain the equilibrium distance, a, separating adjacent dimers along a given helix or layer (Fig. 2a):

$$a = 2r\left[1 + \left(\frac{Sb}{2\pi r}\right)^2\right]\sin\frac{\pi}{N}. \tag{2}$$

As we consider the geometry of the canonical MT, the number of protofilaments is $N = N_0 = 13$ and its radius is $r = r_0$. Furthermore, the canonical MT has 3-start helices of monomers (Chrétien and Wade 1991), which corresponds to $S = S_0 = 2$ helices of dimers. From the helix angle (in the helical structure, the angle between a row of dimers and the horizontal), $\arctan(Sb/2\pi r)$, we calculate the equilibrium distance, d, between adjacent protofilaments, and the equilibrium longitudinal shift, e, between adjacent protofilaments (Fig. 2a):

$$\begin{aligned} d &= a\frac{1}{\sqrt{1+(Sb/2\pi r)^2}} = 2r\sqrt{1 + \left(\frac{Sb}{2\pi r}\right)^2}\sin\frac{\pi}{N}, \\ e &= a\frac{Sb/2\pi r}{\sqrt{1+(Sb/2\pi r)^2}} = \frac{Sb}{\pi}\sqrt{1 + \left(\frac{Sb}{2\pi r}\right)^2}\sin\frac{\pi}{N}. \end{aligned} \tag{3}$$

The notation is as before. Protofilaments interact laterally with a lateral spacing d. Each protofilament is shifted lengthwise by e with respect to its neighbour. Dimensions of the dimer neighbourhood in the lattice are listed in Table 2.

To calculate the position vector, $\mathbf{R_{ij}}$, in the two-dimensional plane, of a dimer that belongs to the protofilament i' and to the layer of dimers j' in a three-dimensional structure representing the canonical MT, we use the mapping

$$f : \{1..N\} \times \mathbb{N} \to \mathbb{R}^2$$

$$(i', j') \mapsto f(i', j') = \mathbf{R_{ij}} = \begin{bmatrix} (j'-1)b + \text{Frac}\left[\frac{i'-1}{N}\right]Ne \\ \text{Frac}\left[\frac{i'-1}{N}\right]Nd \end{bmatrix}. \tag{4}$$

In the three-dimensional helical structure, i' represents the protofilament ($1 \leq i' \leq N$), and j' is the index of the dimer layer in the MT ($1 \leq j'$). In the two-dimensional planar lattice, i is related to the y-position, j to the x-position: the x-axis is parallel to the

Table 2 Parameter values which, used in Eq. 4, give the two-dimensional planar lattices of dimers in accordance with the MT's geometry and with no mismatch as shown in Figs. 1c and 2a

N_0	r_0	S_0	b	Pitch	a	d	e
13	12	2	8	16	6.01	5.88	1.24

N_0 and S_0 represent the number of protofilaments and helices in the canonical MT. Its radius r_0 and the pitch ($S_0 b$) characterize the helices defining the canonical MT. b is the distance between two adjacent subunits along the same protofilament. a, d and e are calculated by Eqs. 2 and 3. Values of r_0, b, pitch, a, d and e are expressed in nanometers

Fig. 1 Geometrical model of a microtubule (*MT*). Here the canonical MT is used as an example. **a** An MT is a long, hollow cylinder with a wall made up of *N* protofilaments consisting of cylindrical tubulin dimers longitudinally stacked. **b** An MT is a three-dimensional helical lattice made up of the centers of mass of the dimers. Centers of mass of the dimers are aligned with a spacing *b* to form the protofilaments that run lengthwise along the wall. Each protofilament is shifted lengthwise with respect to its neighbour describing helical pathways around the MT. Each helix has a radius *r* and a pitch *Sb*, where *S* is the number of helices necessary to describe the whole MT surface. The *grey* and *black helices* depict two helices running around the MT wall. **c** The two-dimensional lattice of dimers: the three-dimensional lattice is longitudinally opened and flattened. *Arrows* represent the protofilament axis
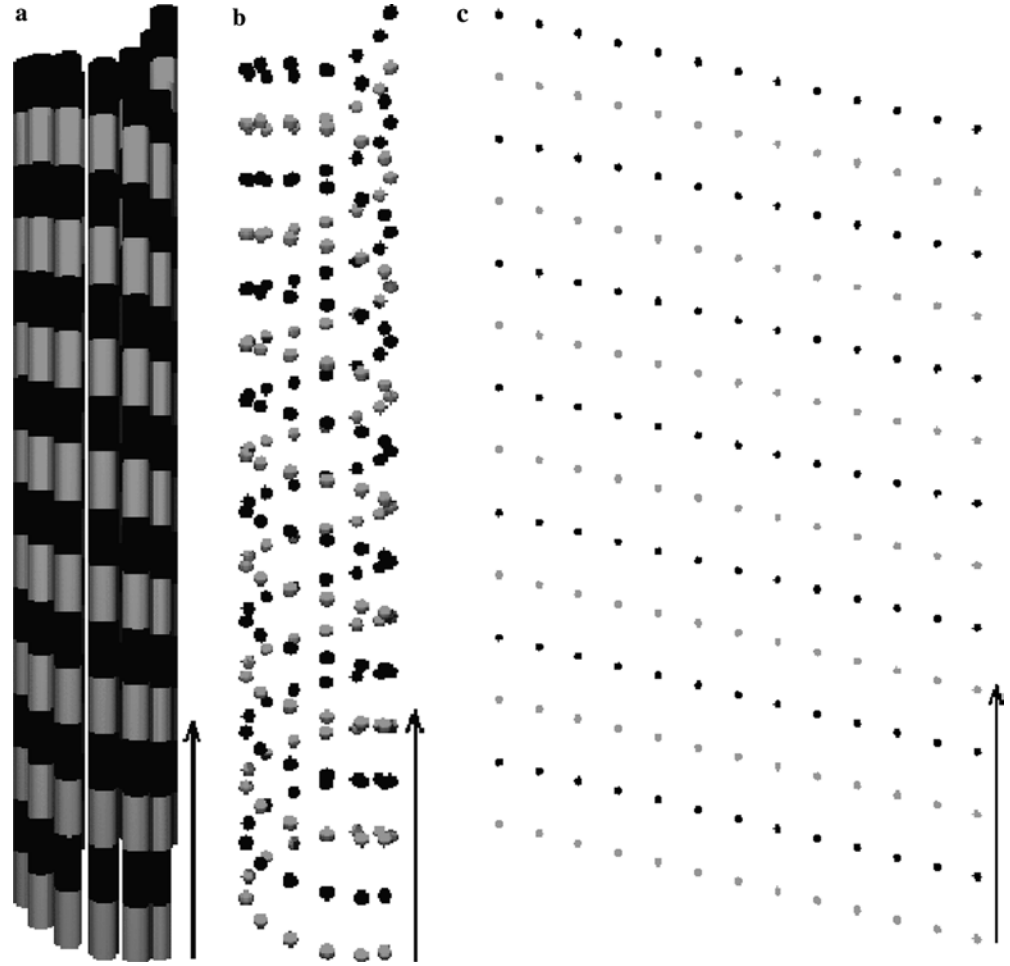
protofilament axis (Fig. 2a). In Eq. 4 the function Frac [·] is the fractional value function; in the first coordinate, it is used to identify the layer, while in the second it designates which protofilament of the MT the particular dimer belongs to. The neighbourhood of a dimer in the three-dimensional helical lattice (Fig. 1b) is preserved in the two-dimensional planar geometry owing to the periodicities implied by the use of the function Frac [·]. Hence, in the two-dimensional planar lattice, for two adjacent dimers $D_{i,j}$ and $D_{i,j+1}$ along the same protofilament, we have $\mathbf{R_{i,j+1}} = \mathbf{R_{i,j}} + \mathbf{b}$, and for two adjacent dimers $D_{i,j}$ and $D_{i+1,j}$ along the same layer or helix, $\mathbf{R_{i+1,j}} = \mathbf{R_{i,j}} + \mathbf{a}$. Subsequently, $\mathbf{R_{i+1,j+1}} = \mathbf{R_{i,j}} + \mathbf{a} + \mathbf{b}$. Vectors **a** and **b** are the lattice vectors, $\|\mathbf{a}\| = a$ and $\|\mathbf{b}\| = b$ (Fig. 2a).

For noncanonical structures, the vector position, $\mathbf{R_{i,j}}$, must be rotated by an angle θ, given in Eq. 1 with the parameters of the dimer lattice to resolve the mismatch induced by extra protofilaments.

Governing equations

By connecting adjacent dimers of the planar lattice by springs with heterogeneous elastic constants (Fig. 2), we model an MT by a lattice with anisotropic elastic properties. This provides a framework to study the vibrational dynamics of dimers within the MT surface.

To study the internal MT dynamics, we model the small displacements of dimers, inside the MT wall, from an equilibrium position. Any stretching or compression of any bond between nearest-neighbour dimers (Fig. 2a) in the lattice will result in a restoring force obeying Hooke's law. We denote the vector displacement, $\mathbf{u}_{i,j}$, of the dimer $D_{i,j}$ in the orthogonal coordinate system (x, y) (Fig. 2a) by

$$\mathbf{u_{i,j}}(\mathbf{t}) = \left[x_{i,j}(t), y_{i,j}(t)\right]^{\mathrm{T}}, \tag{5}$$

where $x_{i,j}(t)$ and $y_{i,j}(t)$ denote small displacements from equilibrium of the dimer, $D_{i,j}$, in the directions along the protofilament (x) and orthogonal to it (y), respectively (Fig. 2a). In the three-dimensional helical structure, $x_{i,j}(t)$ corresponds to longitudinal displacements from equilibrium, and $y_{i,j}(t)$ are analogous to angular displacements (Sirenko et al. 1996a).

As the deviations from equilibrium are small, we approximate the elastic potential energy, $\phi_{i,j}$, of a dimer, $D_{i,j}$, as a harmonic potential. Then, $\phi_{i,j}$, has the form

$$\phi_{i,j} = \frac{1}{2}\sum_{l=-1}^{1}\sum_{m=-1}^{1} k_{i+l,j+m}||\mathbf{u_{i,j}}(t) - \mathbf{u_{i+l,j+m}}(t)||^2 \qquad (6)$$

where $k_{i+l,j+m}$ is the (l,m) element of the contact matrix, $K_{i,j}$, for the dimer, $D_{i,j}$, defined by the neighbourhood system shown in Fig. 2b. Hence, the matrix, $K_{i,j}$, has the form

$$K_{i,j} = \begin{bmatrix} 0 & k_h & k_a \\ k_p & 0 & k_p \\ k_a & k_h & 0 \end{bmatrix}, \qquad (7)$$

where k_h is the elastic constant along the main helix, k_p is the elastic constant along a protofilament, and k_a is the elastic constant along the antihelix (Fig. 2b). The values of the elastic constants k_h, k_p and k_a are assumed to be different from each other. This assumption directly results in an elastic lattice anisotropy that is well documented in the literature (Kis et al. 2002), although precise numerical magnitudes of these constants are yet unknown.

Using Newton's second law of motion and the elastic potential energy Eq. 6, we find the two Cartesian components of the equation of motion for the dimer $D_{i,j}$ to be

Fig. 2 Geometrical characteristics of the planar lattice of dimers. The x-axis is the protofilament axis represented by *arrows* in Fig. 1. **a** Lattice representing the canonical MT, where $a = (e,d)$ and $b = (b,0)$. The longitudinal shift between two adjacent protofilaments is e. Here d represents the distance between two adjacent protofilaments, and b is the distance between two adjacent dimers along a given protofilament. Parameter values are given in Table 2. Bonds in the lattice describe the nearest-neighbour dimers in interaction with a given dimer. **b** The neighbourhood system of a given dimer $D_{i,j}$. **c** The canonical MT lattice is shown in *black* and the lattice for an MT made up of 15 protofilaments and 3 helices (corresponding to the 15-protofilament and 5-start helix MT in the monomer lattice) is in *gray*. To accommodate the two extra protofilaments the lattice is rotated by an angle θ

$$m\frac{\partial^2 x_{i,j}}{\partial t^2} = k_h\left(x_{i-1,j} + x_{i+1,j} - 2x_{i,j}\right) \\ + k_p\left(x_{i,j-1} + x_{i,j+1} - 2x_{i,j}\right) \\ + k_a\left(x_{i-1,j+1} + x_{i+1,j-1} - 2x_{i,j}\right), \qquad (8)$$

and

$$m\frac{\partial^2 y_{i,j}}{\partial t^2} = k_h\left(y_{i-1,j} + y_{i+1,j} - 2y_{i,j}\right) \\ + k_p\left(y_{i,j-1} + y_{i,j+1} - 2y_{i,j}\right) \\ + k_a\left(y_{i-1,j+1} + y_{i+1,j-1} - 2y_{i,j}\right), \qquad (9)$$

where m is the mass of a dimer. From Eqs. 5, 8 and 9 we obtain

$$m\frac{\partial^2 \mathbf{u_{i,j}}}{\partial t^2} = k_h\left(\mathbf{u_{i-1,j}} + \mathbf{u_{i+1,j}} - 2\mathbf{u_{i,j}}\right) \\ + k_p\left(\mathbf{u_{i,j-1}} + \mathbf{u_{i,j+1}} - 2\mathbf{u_{i,j}}\right) \\ + k_a\left(\mathbf{u_{i-1,j+1}} + \mathbf{u_{i+1,j-1}} - 2\mathbf{u_{i,j}}\right). \qquad (10)$$
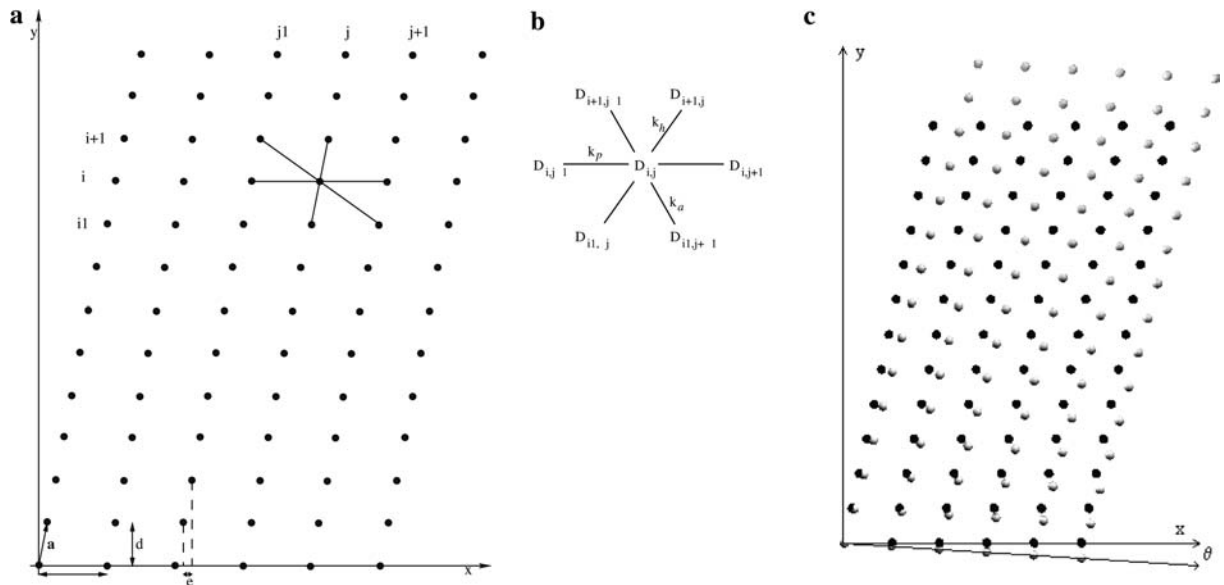
The boundary conditions are $\mathbf{u_{N,j}} = \mathbf{u_{0,j+S}}$, because dimers $D_{N,j}$ and $D_{1,j+S}$ are adjacent along a given helix to preserve the helical pathways running around MTs.

Accordingly we look for wavelike solutions of Eq. 10 of the form

$$\mathbf{u_{i,j}} = \tilde{\mathbf{c}}e^{i(\mathbf{k}\cdot\mathbf{R_{ij}}-\omega t)}, \qquad (11)$$

where $\tilde{\mathbf{c}}$ is an arbitrary vector amplitude, ω a frequency, $\mathbf{k}$ a two-dimensional wave-vector with components k_x and k_y, and $\mathbf{R_{ij}} = [(j-1)b\cos\theta + (i-1)$. $(e\cos\theta - d\sin\theta), (j-1)b\sin\theta + (i-1)$ $(e\sin\theta + d\cos\theta)]^T$ is the position vector of the dimer $D_{i,j}$. Here the position vector, $\mathbf{R_{i,j}}$, results from a rotation of the corresponding canonical structure position vector by angle θ. We substitute Eq. 11 into Eq. 10 to find the associated dispersion relation between ω and $\mathbf{k}$ given by

a

b

c

$$\omega^2 = \frac{2}{m}\Big(k_{\mathrm{h}}\big[1-\cos\left(a[k_x\cos(\alpha+\theta)+k_y\sin(\alpha+\beta)]\right)\big]$$
$$+k_{\mathrm{p}}\big[1-\cos\left(b[k_x\cos\theta+k_y\sin\theta]\right)\big]$$
$$+k_{\mathrm{a}}[1-\cos(k_x(b\cos\theta-a\cos(\alpha+\theta))$$
$$+k_y(b\sin\theta-a\sin(\alpha+\beta)))]\Big). \tag{12}$$

For an $M{\times}N$ orthogonal two-dimensional lattice representing the canonical structure composed of M dimers along the x-direction, and N dimers along the y-direction, the wave-vectors, $\mathbf{k}$, may be defined by (Kittel 1956)

$$k_x = \frac{q\pi}{b(M+1)}, \quad k_y = \frac{p\pi}{a(N+1)}, \tag{13}$$

where $p=1...N$ and $q=1...M$. To consider MTs with a different number of protofilaments we must rotate the wave-vector by an angle θ. So the general expression of the vector, $\mathbf{k}$, is defined by

$$k_x = \frac{q\pi}{b(M+1)}\cos\theta - \frac{p\pi}{a(N+1)}\sin\theta,$$
$$k_y = \frac{q\pi}{b(M+1)}\sin\theta + \frac{p\pi}{a(N+1)}\cos\theta, \tag{14}$$

where θ (see Eq. 1) is the skew angle from the axis of the MT.

For our slanted lattice, the wave-vectors are such that

$$\tilde{k}_x = k_x,$$
$$\tilde{k}_y = k_y\sin\alpha + k_x\cos\alpha, \tag{15}$$

where the angle α is the complementary angle of the helix angle, $\alpha = (\pi/2) - \arctan(Sb/2\pi r)$. The component $\tilde{k}_x$ is related to the protofilament direction, and $\tilde{k}_y$ is related to the orientation of helices. The parameter M is proportional to the number of helices, S, running around the MT wall.

Substituting the previous expressions from Eqs. 14 and 15 into Eq. 12 gives the dispersion relation between ω and $\tilde{\mathbf{k}}$:

$$\omega_{p,q}^2 = \frac{2}{m}\Bigg[k_{\mathrm{h}}\bigg[1-\cos\bigg(a\bigg[\bigg(\frac{q\pi}{b(M+1)}\cos\theta - \frac{p\pi}{a(N+1)}\sin\theta\bigg)\cos(\alpha+\theta)$$
$$+ \bigg(\frac{q\pi}{b(M+1)}\sin\theta + \frac{p\pi}{a(N+1)}\cos\theta\bigg)\sin(\alpha+\theta)\bigg]\bigg)\bigg]$$
$$+ k_{\mathrm{p}}\bigg[1-\cos\bigg(b\bigg[\bigg(\frac{q\pi}{b(M+1)}\cos\theta - \frac{p\pi}{a(N+1)}\sin\theta\bigg)\cos\theta$$
$$+ \bigg(\frac{q\pi}{b(M+1)}\sin\theta + \frac{p\pi}{a(N+1)}\cos\theta\bigg)\sin\theta\bigg]\bigg)\bigg]$$
$$+ k_{\mathrm{a}}\bigg[1-\cos\bigg(\bigg(\frac{q\pi}{b(M+1)}\cos\theta - \frac{p\pi}{a(N+1)}\sin\theta\bigg)(b\cos\theta - a\cos(\alpha+\theta))$$
$$+ \bigg(\frac{q\pi}{b(M+1)}\sin\theta + \frac{p\pi}{a(N+1)}\cos\theta\bigg)(b\sin\theta - a\sin(\alpha+\theta))\bigg)\bigg]\Bigg]. \tag{16}$$

For small p,q we note that $\omega_{p,q}\to 0$ in Eq. 16. They therefore represent acoustic vibrational modes.

By estimating the gradient of $\omega_{p,q}$ in specific directions, we obtain the group velocity of vibrations propagating along the protofilament and along the helix. The velocity of longitudinal vibrations along protofilaments is

$$v_x = \sqrt{\frac{1}{m}\Big(k_{\mathrm{h}}a^2(\cos(\alpha+\theta)-\cot\alpha\sin(\alpha+\theta))^2}$$
$$+ k_{\mathrm{p}}b^2(\cos\theta - \cot\alpha\sin\theta)^2$$
$$+ k_{\mathrm{a}}(b\cos\theta - a\cos(\alpha+\theta)$$
$$- \cot\alpha(b\sin\theta - a\sin(\alpha+\theta)))^2\Big)^{1/2}. \tag{17}$$

The velocity of vibrations along the helix is

$$v_y = \frac{a}{d}\sqrt{\frac{1}{m}}\big\{k_{\mathrm{h}}a^2\sin^2(\alpha+\theta) + k_{\mathrm{p}}b^2\sin^2\theta$$
$$+ k_{\mathrm{a}}[b\sin\theta - a\sin(\alpha+\theta)]^2\big\}^{1/2}. \tag{18}$$

The velocities of vibrations (along protofilaments and along helices) depend on the elastic constants, k_{p}, k_{h} and k_{a}, and the mass, m, of tubulin dimers. They also depend on the structural properties of MTs determined by the skew angle θ and the helix angle α. In the three-dimensional helical structure, at a macroscopic level, the longitudinal vibrations along protofilaments correspond to longitudinal vibrations of the MT, and vibrations along helices to torsional vibrations of the MT.

Results

Elastic constants

Longitudinal interactions between dimers have polar, hydrophobic and electrostatic components (Nogales et al. 1998). The contact interface is highly complementary in shape; hence, van der Waals interactions are important. Lateral interactions (between α–α and β–β) have more important electrostatic character than longitudinal interactions (Nogales et al. 1999). The lat-
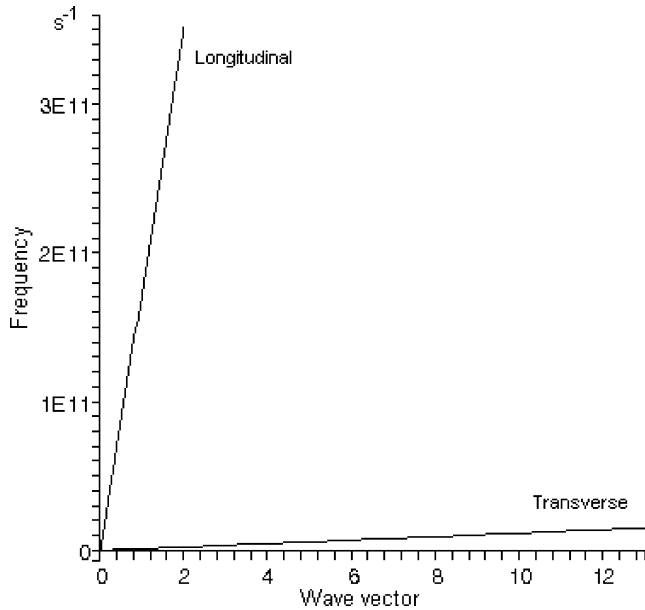
Fig. 3 Dispersion relations for the canonical MT. The curve labeled *Longitudinal* represents the dispersion relation for vibrations propagating along protofilaments. Frequencies can yield 3×10^{11} 1/s. The curve labeled *Transverse* is the dispersion relation for vibrations propagating along helices. Frequencies can reach 5×10^{10} 1/s

eral contacts between tubulin dimers in neighbouring protofilaments have a decisive role for MT dynamics, stability, rigidity and architecture (Meurer-Grob et al. 2001; Nogales et al. 1999). Tubulin dimers are relatively strongly bound in the longitudinal direction (along protofilaments), while the lateral interaction between protofilaments is much weaker (Kis et al. 2002; Nogales 1999; Sept et al. 2003); hence, $k_p > k_h, k_a$. While all the longitudinal intraprotofilament interactions are assumed to be the same, the lateral interactions between the protofilaments are known to be different (Li et al. 2002) depending on direction; hence, $k_h \neq k_a$.

Tuszynski et al. (2005) have done molecular dynamics computations to study the electrostatic properties of tubulin heterodimers. Sept et al. (2003) performed a computation of the protofilament–protofilament binding free energy as a function of the longitudinal shift along the protofilament axis. The data published in this latter work indicate the presence of two stable equilibrium positions that correspond to MT lattice types A and B. They also discriminate the polar and electrostatic contribution to the free binding energy. We have processed the potential diagram published by Sept et al. (2003) in their Fig. 1 in order to evaluate the corresponding elastic coefficient in a harmonic approximation around the potential minimum. We found the value to be $k \simeq 4$ N/m.

De Pablo et al. (2003) estimated experimentally by radial indentation of MTs with a scanning force microscope tip an elastic constant value related to lateral interactions between protofilaments. Indentations, induced by the nanometer-sized tip positioned on the top

of an MT, result in a linear elastic response with the elastic constant $k = 0.1$ N/m.

The estimate of Sept et al. (2003) corresponds to interactions between two protofilaments when one is slid along its length against the other that is kept fixed, the protofilament–protofilament shift along the protofilament axis. However, the estimates of de Pablo et al. (2003) correspond to a radial dependence of the force on the distance to the centre of the MT.

Vibration dynamics

While we have no direct experimental evidence at present to claim the anisotropy in the elastic coefficients k_a, k_h and k_p, it is more prudent to allow these parameters to differ from each other. To approximately represent the anisotropy, we judiciously chose $k_p = 4.5$ N/m, $k_h = 0.1$ N/m and $k_a = 0.01$ N/m. The mass of the dimer is taken to be $m = 1.83 \times 10^{-22}$ kg.
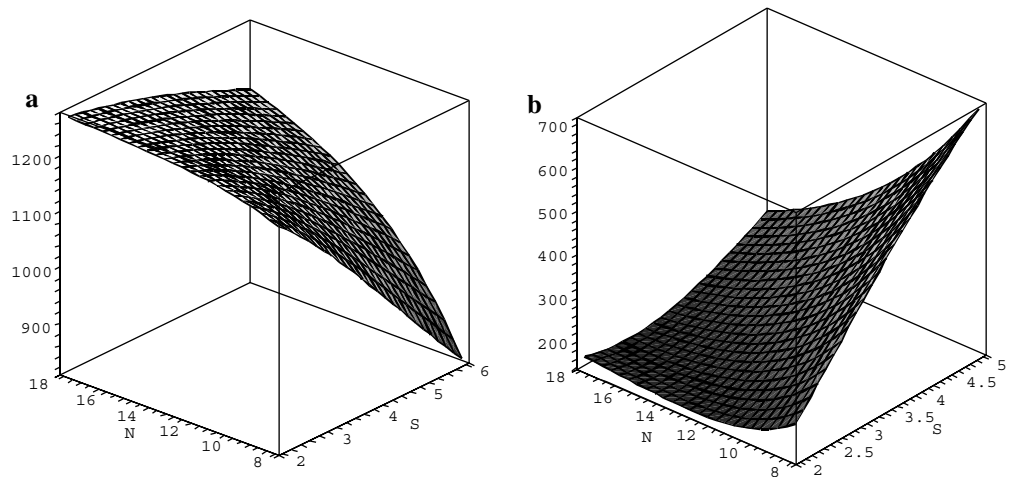
Dispersion relations along the protofilament and helix directions are represented in Fig. 3. Frequencies reach 3×10^{11} 1/s along the protofilament direction, and only 5×10^{10} 1/s along the helix direction. Both longitudinal and transverse modes are acoustical (Fig. 3). The corresponding propagation velocities range between 145 and 1,260 m/s, where the smallest velocity is related to the helix direction and the largest to the protofilament direction. The range of propagation velocities is in accordance with the previously predicted values (Pokorny et al. 1997; Sirenko et al. 1996a, 1996b). Our frequencies are slightly higher than the predicted frequencies of Pokorny et al. (1997) (Table 1). These results, however, are still subject to experimental determination. It is noteworthy that the vibrations which propagate along the protofilament do so significantly faster than those along the helix, $v_x > v_y$ (Table 3).

Table 3 Estimates of frequencies ω, velocities v and wavelengths λ along the protofilament direction (labelled x) and along the helical pathway (labelled y) for four MTs

$S=2$			
A	$N=13$	$\omega_x = 3.15 \times 10^{11}$ 1/s	$\omega_y = 4.8 \times 10^{10}$ 1/s
		$v_x = 1,256$ m/s	$v_y = 147$ m/s
		$\lambda_x = 3.9 \times 10^{-9}$ m	$\lambda_y = 3 \times 10^{-9}$ m
B	$N=15$	$\omega_x = 3.15 \times 10^{11}$ 1/s	$\omega_y = 5 \times 10^{10}$ 1/s
		$v_x = 1,237$ m/s	$v_y = 151$ m/s
		$\lambda_x = 3.9 \times 10^{-9}$ m	$\lambda_y = 3 \times 10^{-9}$ m
$S=3$			
C	$N=13$	$\omega_x = 3.15 \times 10^{11}$ 1/s	$\omega_y = 4.8 \times 10^{10}$ 1/s
		$v_x = 1,222$ (m/s)	$v_y = 197$ (m/s)
		$\lambda_x = 3.8 \times 10^{-9}$ m	$\lambda_y = 4.1 \times 10^{-9}$ m
D	$N=15$	$\omega_x = 3.15 \times 10^{11}$ 1/s	$\omega_y = 5 \times 10^{10}$ 1/s
		$v_x = 1,263$ m/s	$v_y = 167$ m/s
		$\lambda_x = 4 \times 10^{-9}$ m	$\lambda_y = 3.3 \times 10^{-9}$ m

A the canonical MT ($N=13$ and $S=2$), *B* the MT with 15 protofilaments and 2 helices, *C* the MT with 13 protofilaments and 3 helices [3 helices in the dimer lattice corresponds to 5-start helices in the monomer lattice (Chrétien et al. 1998)] and *D* the MT with 15 protofilaments and 3 helices

Fig. 4 The effects of structural parameters on vibration velocities along the protofilament and helix directions. Velocities of vibrations, v_x and v_y, as a function of the number of protofilaments and of helices, along the protofilament and helix directions, respectively

In Fig. 4 we represent the effects of the structural properties of MTs (number of protofilaments and helices) on the vibration velocities. The vibration velocities along the protofilament and helix directions are very sensitive to the number of protofilaments and to the number of helices. The number of helices, S, has a larger influence than the number of protofilaments. Furthermore S has a major influence when the number of protofilaments is very small, i.e., $N=8$.

In Table 3 we give our estimates of the frequencies, velocities and wavelengths along the direction of the protofilaments and of the helices.

Discussion

From the helical structure of MTs, we developed a planar lattice of dimers that are considered to be coupled oscillators vibrating about equilibrium positions. The use of a discrete model was necessary to obtain vibration dispersion relations accounting for the geometrical properties of MTs and particulars of protein–protein interactions. Our planar lattice of dimers without a seam respects the geometrical properties of MTs. Equations of motion for dimers were derived and an ansatz of harmonic solutions found which satisfy the periodic boundary conditions. We obtained dispersion relations for a number of vibrational acoustic modes and the corresponding propagation velocities. We give explicit expressions for vibration frequencies and velocities, along both protofilament and helix directions. These quantities are functions of only elastic constants and structural parameters of MTs.

Thus, from the planar lattice we are able to study vibration modes of dimers along protofilament and helix directions, which respectively correspond to the longitudinal and torsional modes of vibrations of dimers inside the MT wall. It is noteworthy that the vibrations which propagate along the protofilament do so significantly faster than those along the helix. We also observe a strong dependence of the microscopic vibra-

tional properties of MTs on the number of protofilaments and of helices. Finally, our predicted vibrational frequencies and corresponding velocities are in the same range as those estimated by Sirenko et al. (1996a, 1996b), and slightly larger than those estimated by Pokorny et al. (1997) (Table 1).

This work was possible owing to a recently obtained experimental body of data coming from several groups and describing a number of physical and structural properties of MTs (de Pablo et al. 2003; Kis et al. 2002; Nogales 1999; Sept et al. 2003). The most marked aspect of MTs observed was the anisotropic character of MT elasticity that is reflected in the heterogeneity of elastic coefficients. Theoretical estimates of the elastic constants required knowledge of the tubulin dimer–dimer interaction potential or relevant experimental data. With the knowledge of particular interaction strengths between two neighbouring dimers, resulting from the protofilament–protofilament shifting along the MT axis (Sept et al. 2003) or during the radial indentations of MTs (de Pablo et al. 2003), as guidance, we obtained rough estimates of the molecular elastic constants along three different directions on the MT surface. These values were used for the modeling of the vibrational dynamics.

In this work we were guided by earlier works that explored both the continuum medium approach to a cylindrical hollow structure (Sirenko et al. 1996a) and a one-dimensional approximation to the calculation of phonon dispersion (Pokorny et al. 1997). Nevertheless, we believe that neither the continuum model nor the one-dimensional approximation is adequate owing to the heterogeneity of the MT structure. However, the knowledge of several modes of vibration as well as the predicted dispersion relations and phonon velocities were very useful in our modeling. The radial motions are not described in our model (Sirenko and Dutta 2001). In terms of the continuum medium approximation, our MT would be a cylinder with a fixed radius.

The viscosity of the surrounding solution (in vitro) or of cytoplasm (in vivo) may affect vibrations by damping them out (Foster and Baish 2000). Foster and Baish

calculated the relaxation time caused by viscous damping to be in the nanosecond region. For our smallest predicted frequency, we obtain a period 2 orders of magnitude smaller than the relaxation time. Furthermore, Pokorny (2004) has shown that the viscous damping effects due to the cytoplasm viscosity can be minimized by the ion condensation around the MT. Thus, in our model, the viscous damping effects are neglected.

Our lattice of dimers without mismatch can be classified as a B-type lattice where lateral contacts are made between α–α and β–β subunits. This lattice type is predominantly observed in MT structures; however, MTs can possess a seam in which lateral contacts exist between heterologous subunits. In our dynamical model, the seam could be described by different elastic constants for the boundary nodes to model differences of energy occurring at these contacts. But no change will occur in the geometrical model. This aspect still requires further attention.

References

Amos LA (1995) Trends Cell Biol 5:48
Boal D (2002) Mechanics of the cell. Cambridge University Press, London
Chrétien D, Wade R (1991) Biol Cell 71:161
Chrétien D, Flyvbjerg H, Fuller SD (1998) Eur Biophys J 27:490
de Pablo PJ, Schaap IAT, MacKintosh FC, Schmidt CF (2003) Phys Rev Let 91:098101
Foster KR, Baish JW (2000) J Biol Phys 26:255
Janmey PA, Euteneuer U, Traub P, Schliwa M (1991) J Cell Biol 113:155
Jánosi IM, Chrétien D, Flyvbjerg H (1998) Eur Biophys J 27:501
Kis A, Kasas S, Babic B, Kilik AJ, Benoit W, Briggs GAD, Schonenberger C (2002) Phys Rev Lett 89:248101
Kittel C (1956) Introduction to solid state physics. Wiley, New York
Langford GM (1980) J Cell Biol 87:521
Li H, DeRosier DJ, Nicholson WV, Nogales E, Downing KH (2002) Structure 10:1317
Meurer-Grob P, Kasparian J, Wade RH (2001) Biochemistry 40:8000
Metoz F, Wade RH (1997) J Struc Biol 118:128
Nogales E, Wolf S, Downing K (1998) Nature 391:199
Nogales E (1999) CMLS 5:133
Nogales E, Whittaker M, Miligan RA, Downing KH (1999) Cell 96:79
Pokorny J, Jelinek F, Trkal V, Lamprecht I (1997) Astrophys Space Sci 23:171
Pokorny J (2004) Bioelectrochemistry 63:321
Ray S, Meyhofer E, Miligan RA, Howard J (1993) J Cell Biol 121:1083
Sept D, Baker NA, McCammon JA (2003) Protein Sci 12:2257
Sirenko YM, Stroscio MA, Kim KW (1996a) Phys Rev E 54:1816
Sirenko YM, Stroscio MA, Kim KW (1996b) Phys Rev E 53:1003
Sirenko YM, Dutta M (2001) Phonons in nanostructures. Cambridge University Press, London
Tolomeo JA, Holley MC (1997) Biophys J 73:2241
Tuszynski JA, Brown JA, Crawford E, Carpenter EJ, Nip MLA, Dixon JM, Sataric MV (2005) Math Comp Model (to appear)
Unger E, Bohm KJ, Vater W (1990) Electron Microsc Rev 3:355
VanBuren V, Odde DJ, Cassimeris L (2002) Proc Natl Acad Sci USA 9:6035